## **CHAPTER 50**

# Improvement of Submerged Doppler-Type Directional Wave Meter and its Application to Field Observations

Noriaki Hashimoto<sup>1</sup>, Masao Mitsui<sup>2</sup>, Yoshimi Goda<sup>3</sup>, Toshihiko Nagai<sup>4</sup>, and Tomoharu Takahashi<sup>5</sup>

#### Abstract

This paper presents an improved submerged Doppler-type directional wave meter which has the capability of measuring water surface elevations and multiple current velocity components. These components are determined from Doppler frequency shifts of ultrasonic waves in water. The improved system has proven to be capable of successfully obtaining tide, current and directional wave data. In addition, this directional wave meter has accurately estimated directional wave spectra in severe sea conditions with the use of some techniques introduced in this paper.

#### 1. Introduction

Field studies in coastal areas are indispensable not only for scientific research but also for pre- and post-construction monitoring of the effects of engineering projects. Particularly for the latter cases, field surveys often require not only a long observation period but also require the measurement of many parameters such as waves, currents, and tides to clarify the mutual interaction between those natural conditions and human activities. Many types of observational devices have been developed and improved on over the years. Most of them, however, were designed to measure specific parameters separately using their own techniques. To obtain meaningful results, it is necessary to measure the sea conditions comprehensively, i.e., the measurement of

<sup>&</sup>lt;sup>1</sup> Chief, Hydrodynamics Lab., Marine Environment Div., Port and Harbour Research Institute (PHRI), Ministry of Transport, 1-1-3 Nagase, Yokosuka 239, Japan.

<sup>&</sup>lt;sup>2</sup> Member, Research and Development Division, Kaijyo Corporation,3-1-5 Sakae-cho,Hamura Tokyo 205, Japan.

<sup>&</sup>lt;sup>3</sup> Professor, Department of Civil Engineering, Yokohama National Universitity, Hodogaya-ku, Yokohama 240, Japan.

<sup>&</sup>lt;sup>4</sup> Chief, Marine Observation Lab., Hydraulic Engineering Div., PHRI.

Managing Director, Japan Marine Surveyors Association, 14-12 Kodenma-cho, Nihonbashi, Chuo-ku, Tokyo 103, Japan.

many parameters at the same time and at the same location, because each item is mutually and closely interrelated.

Until recently, a simple instrument for directional seas has not yet been developed. In Japan, the commonly used wave meter is a submerged ultrasonic-type wave gage (USW) which can be installed in maximum water depths of 50m. A submerged ultrasonic-type current meter (CWD) has also been developed for measuring directional seas but it is limited to applications with maximum water depths of about 30m because of the decay of water particle velocities due to depth. For these reasons, the development of a well-combined measurement system has been anticipated in Japan.

With this background, we developed the submerged Doppler-type directional wave meter and introduced it at ICCE `94 in Kobe. This system, known as the DWM, is extremely convenient since it is a single instrument that can be used to obtain accurate observations of directional seas. It is considered to be one of the most useful measuring systems for investigating directional seas.

Since ICCE '94, further improvements have been made to the DWM and additional field experiments have been conducted to enhance the performance of the DWM from many aspects. In this paper, we introduce new features of the DWM-II (the improved DWM is hereafter called the DWM-II) with its validity and applicability demonstrated with experimental results. Some techniques for improving the performance of the DWM-II are also presented along with the results of field experiments.

#### 2. System Description

An improved "submerged Doppler-type directional wave meter", the DWM-II, possesses the multiple functions of a wave meter, current meter and tide gage. The main components of the system are a submerged transducer, measurement section, and computation unit. The transducer is supported with gimbals and has oscillators which operate four acoustic beams. One beam is vertically directed and operates at a frequency of 200 kHz. The other three acoustic Doppler current profiler (ADCP) beams operate at a frequency of 500 kHz, each of which has an inclination of 30 degrees to the vertical.

To measure the water surface elevation, the transducer transmits upward-directed ultrasonic waves and receives that portion of the energy which is reflected off of the water surface. The water surface elevation is estimated by using the ultrasonic wave propagation time based on the known propagation speed in water.

By also transmitting ultrasonic waves upward in three directions, separated by an inclination of 30 degrees, current velocity components,  $U_1(t)$ ,  $U_2(t)$ ,  $U_3(t)$ , can be measured by receiving the acoustic waves reflected back from selected layers of water. The water particle velocity of each layer is estimated from the frequency shift caused

by the Doppler effect between the transmitted waves and the reflected waves. Using a time sharing system, all measurements are made every 0.125 seconds or at a sampling frequency of 8 Hz.

In addition, the DWM-II is equipped with a pressure sensor, compass and inclinometer in the transducer. These are used to monitor the conditions of the DWM-II itself and to check the quality of the measured data.

## 3. Field Testing

Field testing was carried out from August 1993 to March 1995 off the entrance of Kamaishi Port, as shown in **Figure 1**, where the conventional ultrasonic wave meter (USW) has been operational since 1983. The transducer of the DWM-II was positioned about 100m away from the USW at a height of 1.5m above the seabed where the water depth is 48m. The time series data consisted of water surface elevation and current velocity components that were measured at three different water depths of 10m, 23m and 38m below the water surface. These data were recorded on an optical magnetic disk at a sampling rate of 2 Hz for 20 minutes every two hours. Some statistical parameters, including the directional spectrum, were computed immediately after each observation and were recorded on the optical magnetic disk. In addition, a rotor-type current meter (RCM) was moored to a float and positioned 100m away to examine the validity of the DWM-II by comparing the results of both meters.

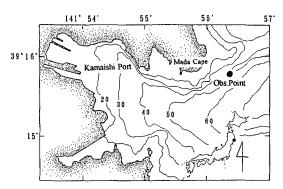


Figure 1 Field Observation Locations

# 4. Examples of Observational Results

Figure 2 shows some examples of the DWM-II time series of wave parameters such as significant wave height  $H_{1/3}$ , significant wave period  $T_{1/3}$ , mean wave direction  $\overline{\theta}$ , peak wave direction  $\theta_p$ , mean spreading angle  $\theta_\kappa$ , and long-crestedness parameter  $\gamma$ .

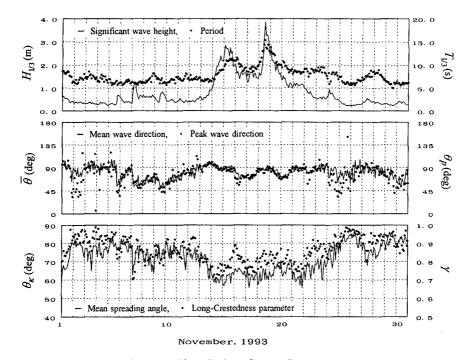


Figure 2 Time Series of Wave Parameters

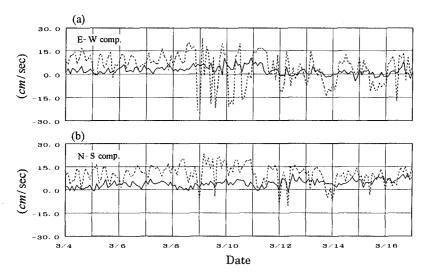


Figure 3 Time Series of the East-West and North-South Current Velocity Components by the DWM-II (solid line) and the RCM(dashed line)

Results have shown that wave parameters, such as significant wave height and period, measured by the DWM-II, show good agreement with those obtained by the USW. The current velocities, however, measured by the DWM-II, are very different than those obtained by the RCM as shown in Figure 3. It is important to note that the RCM is very vulnerable to the current induced by waves and, in fact, moves following the wave motions. This is demonstrated in Figure 4. The existing reports on the currents around the observation site show that the currents there are weak, i.e., 10 cm/s or less, which is consistent with the results of the DWM-II which are also shown in Figure 4. Figure 5 shows the spectra of the currents of the east-west and north-south components measured by the DWM-II at the upper layer 10m below the mean free surface. As shown in Figure 5, two predominant tidal periods can be seen at the diurnal and the semi-diurnal frequencies. These predominant peaks were not observed in the spectra obtained by the RCM due to the limitations already discussed. Therefore, the DWM-II has an advantage over the RCM of measuring intrinsic current fields since it is relatively unaffected by waves.

Figures 6 (a) and (b) show the comparison of the tide level measurements obtained by a tide gage and estimates from the ultrasonic wave data and pressure data of the DWM-II, respectively. Three minute long ultrasonic measurements were made of the mean free surface every two hours at a sampling frequency of 2 Hz. The tide level was obtained by averaging each record. Pressure samples were obtained with the same sampling scheme. Corrections, with respect to the atmospheric pressure measured about 30km away from the observation site, were made to the tide level estimated by the pressure data. Both figures show high correlation.

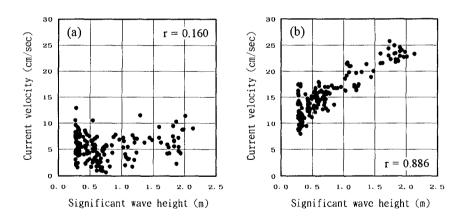


Figure 4 Significant Wave Height and Current Velocity Correlation Measured by the DWM-II (a) and the RCM (b)

Furthermore, Figure 7 shows the relationship between the atmospheric pressure obtained from a barometer 30km away and the estimated atmospheric pressure from the DWM-II. Since the DWM-II pressure sensor measures the combined atmospheric pressure and hydrostatic pressure, the atmospheric pressure can be obtained by taking the difference between ultrasonic tide level data (hydrostatic pressure) and total pressure data. As seen in this figure, there was considerably high correlation. The fact that the atmospheric pressure can be estimated by the DWM-II, with a high degree of accuracy, further demonstrates the high quality of water surface elevation and water pressure data obtained by the DWM-II.

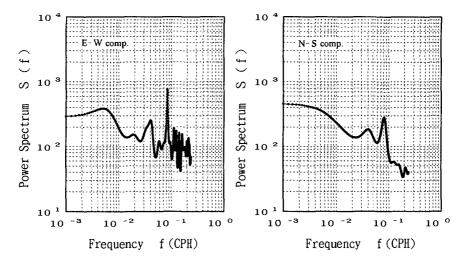


Figure 5 Spectra of the East-West and North-South Current Velocity Components measured by the DWM-II

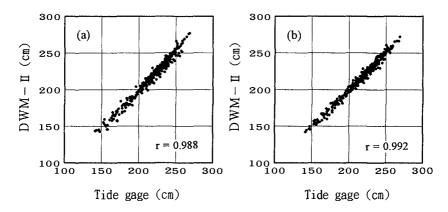


Figure 6 Comparison of Tide Level Measurements

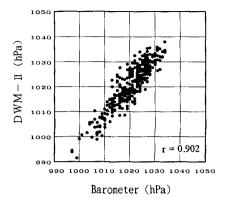


Figure 7 Comparison of Atmospheric Pressure Measurements

## 5. Proposed Techniques for Improving the Performance of the DWM-II

During this study to enhance the performance of the DWM-II, some new techniques have been introduced to mitigate some of its shortcomings. These techniques are presented in the following three sections.

#### 5.1 Estimation of the Principal Wave Direction With Covariances

A disadvantage of measuring directional seas using wave arrays is that waves with lengths L less than two times the minimum separation distance,  $D_{\min}$ , of the array can not be analyzed to produce a directional spectrum. That is, if we wish to analyze waves of length L, the requirement of  $2D_{\min} \leq L$  must be satisfied. However, if we measure x- and y-components such as  $(u\,,v)$  or  $(\eta_x\,,\eta_y)$  related to random wave motions in the same location, we can estimate the representative wave direction using the covariance method described below without being subjected to the above restriction on array spacing.

Longuet-Higgins defined the principal wave direction  $\theta_p$  as the direction along which the root-mean-square (RMS) wave number is the largest or the wave crests are the densest. This can be expressed by the following relationship:

$$\theta_p = \frac{1}{2} \tan^{-1} \frac{2M_{11}}{M_{20} - M_{02}} \tag{1}$$

where the spectral moment  $M_{pq}$  of equation (1) can be evaluated by the following equation:

$$M_{pq} = \int_0^\infty \int_{-\pi}^\pi S(f,\theta) k^{p+q} \cos^p(\theta) \sin^q(\theta) d\theta df$$
 (2)

The spectral moment defined by equation (2) can be alternatively evaluated with the covariance between the time series of several wave motion parameters (Goda, 1982).

By using covariances such as  $\overline{u^2}$ ,  $\overline{v^2}$ , and  $\overline{uv}$ , the principal wave direction can be defined by:

$$\theta_p = \frac{1}{2} \tan^{-1} \frac{2uv}{u^2 - v^2}$$
 (3)

The *i*-th water particle velocity component  $U_i$  measured by the DWM-II is expressed by:

$$U_i = a_i u + b_i v + c_i w (4)$$

where u, v, and w are the orthogonal components of the water particle velocities at the measuring location  $U_i$  and  $a_i$ ,  $b_i$  and  $c_i$  are the coefficients expressed by the following equations:

$$a_{i} = \sin \alpha_{i} \cos \beta_{i}$$

$$b_{i} = \sin \alpha_{i} \sin \beta_{i}$$

$$c_{i} = \cos \alpha_{i}$$

$$(5)$$

where  $\alpha_i$ , and  $\beta_i$  are the angles shown in **Figure 8**. Then the covariance of  $U_i$  is expressed by:

$$\overline{U_i^2} = a_i^2 \overline{u^2} + b_i^2 \overline{v^2} + c_i^2 \overline{w^2} + 2a_i b_i \overline{uv} + 2b_i c_i \overline{vw} + 2a_i c_i \overline{uw}$$
 (6)

That is, the covariance  $\overline{U_i^2}$  is expressed by the six independent covariances such as  $\overline{u^2}$ ,  $\overline{v^2}$ ,  $\cdots$ ,  $\overline{uw}$ . From the linear wave theory, however,

$$\overline{uw} = \overline{vw} = 0 \tag{7}$$

Therefore, Equation (6) reduces to;

$$\overline{U_i^2} = a_i^2 \overline{u^2} + b_i^2 \overline{v^2} + c_i^2 \overline{w^2} + 2a_i b_i \overline{uv}$$
 (8)

In addition to equation (8), since the DWM-II measures free surface displacement  $\eta(t)$ , the covariances  $\overline{w^2}$  can be estimated with the linear wave theory by the following equation:

$$\overline{w^2} = \int_0^\infty S_w(f) df = \int_0^\infty |H_w(f)|^2 S_\eta(f) df$$
 (9)

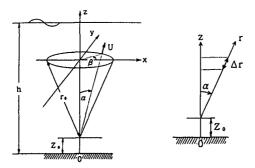


Figure 8 Definition of Coodinate System

where  $S_{w}(f)$  is the power spectrum of the vertical component of water particle velocity w(t),  $S_{\eta}(f)$  is the power spectrum of the free surface displacement  $\eta(t)$  and  $H_{w}(f)$  is the transfer function from w(t) to  $\eta(t)$ .

Finally, the following simultaneous equations, with respect to the unknown values  $\overline{u^2}$ ,  $\overline{v^2}$  and  $\overline{uv}$  can be obtained:

$$\begin{pmatrix} a_1^2 & b_1^2 & 2a_1b_1 \\ a_2^2 & b_2^2 & 2a_2b_2 \\ a_3^2 & b_3^2 & 2a_3b_3 \end{pmatrix} \begin{pmatrix} \overline{u^2} \\ \overline{v^2} \\ \overline{uv} \end{pmatrix} = \begin{pmatrix} \overline{U_1^2} - c_1^2 \overline{w^2} \\ \overline{U_2^2} - c_2^2 \overline{w^2} \\ \overline{U_3^2} - c_3^2 \overline{w^2} \end{pmatrix}$$
(10)

By solving this set of simultaneous linear equations, the principal wave direction can be determined from the definition of Equation (3).

By using these techniques and measuring the water particle velocities, the DWM-II can estimate the principal wave direction,  $\theta_p$ , even in calm sea conditions. This means that even in short wave environments the principal wave direction can be estimated without being restricted by the minimum array spacing requirement. **Figure 9** shows examples of the comparison of the estimated principal wave directions (solid vertical line) and the directional spectra. It can be seen that the estimated principal wave directions compare favorably with the peak energy direction of the directional spectra.

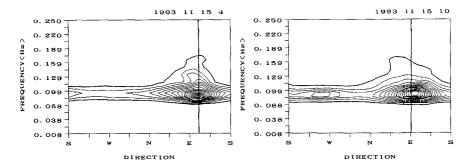


Figure 9 Principal Wave Direction (solid line) and the Directional Spectrum Measured by the DWM-II

#### 5.2 Surface wave Recovery From Subsurface Pressure Records

A disadvantage of utilizing ultrasonic waves in water is that they are severely scattered and absorbed by bubbles when the free surface is disturbed by strong winds or breaking waves. To overcome this limitation, the DWM-II measures pressure as an auxiliary parameter. A proper transformation can be performed to obtain surface wave information from subsurface pressure records. Although many researchers have

gone to great lengths to investigate the possibility of generating surface wave information from subsurface pressure records, and many methods have been proposed to date, almost all of the existing methods are supplemented with various empirical corrections.

Recently, we investigated the relationship between surface waves and subsurface pressure records in detail on the basis of weakly nonlinear directional wave theory. From this investigation we were able to propose a practical method to recover surface wave information by utilizing the shape of the subsurface pressure records. The use of directional spectra information is not required for this new method. This method can be applied for the recovery of surface waves by the DWM-II. The details of these techniques will appear in a paper soon to be published but an outline of this research and methods is presented below.

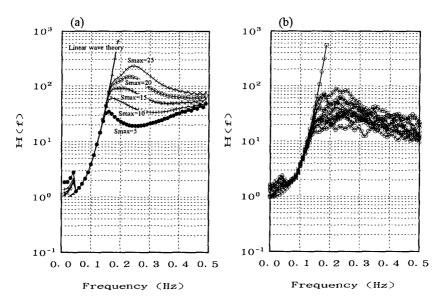


Figure 10 Examples of Theoretical (a) and Observed (b) Transfer Functions H(f) in Water Depth of 50 Meters

Figures 10 (a) and (b) show examples of theoretical and observed transfer functions, H(f), respectively, given by the square root of the ratio  $S_{\eta}(f)/S_p(f)$  where  $S_{\eta}(f)$  is the power spectrum of the water surface elevation and  $S_p(f)$  is that of the subsurface pressure. Note the favorable comparison between the theoretical and observed transfer functions. The Bretscheider-Mitsuyasu type power spectrum and Mitsuyasu type directional spreading function are assumed for the directional spectrum of linear waves. As seen in the figures, the transfer function shows peculiarity in its lower and higher frequency ranges. The characteristics of the transfer functions in those ranges are dependent on the angular spreading parameter,

 $S_{\max}$ , of the directional spectrum and can be successfully explained on the basis of weakly nonlinear directional wave theory. This is due to the fact that k is a vector and  $\omega$  is a scalar. That is to say, the second order nonlinear effect is a function of the wave propagation direction of each linear component wave. Therefore, accurate surface wave recovery, including the high frequency range, requires information of the directional spectrum. The wider the angular spreading function becomes, the greater the difference between the transfer function of the linear wave theory and that of the weakly nonlinear directional wave theory. However, by properly analyzing the shape of the subsurface pressure spectrum, sufficient information can be obtained to accurately recover the surface waves without obtaining the surface directional spectrum.

The proposed method is quite reliable for estimating a wide range of wave heights and periods for both calm and severe sea states.

## 5.3 Surface Wave Recovery from Current Velocity Component Records

In addition to recovering surface waves from subsurface pressure records, the DWM-II is capable of measuring surface waves, without obtaining information about the free surface displacement,  $\eta(t)$ , by properly transforming current velocities at several layers. This is useful since quite frequently, the ultrasonic waves used for measuring  $\eta(t)$  are scattered and absorbed by bubbles at the surface.

The DWM-II can estimate the directional spreading function,  $G(\theta|f)$ , from a set of three current velocities,  $U_1(t)$ ,  $U_2(t)$  and  $U_3(t)$  without information about the free surface displacement,  $\eta(t)$ .

$$G(\theta|f) = \frac{\kappa}{H^{*t} \Phi^{-1} H}$$
 (11)

where  $\kappa$  is a proportionality constant ensuring that  $G(\theta|f)$  satisfies

$$\int_{-\pi}^{\pi} G(\theta|f) d\theta = 1 \tag{12}$$

**H** is the matrix comprised of the transfer functions from the *i*-th current velocity,  $U_i(t)$ , to the free surface displacement,  $\eta(t)$ , and is given by:

$$H_{U_{i}} = \frac{-i\omega \exp(-i\omega\Delta t)}{\Delta r k \sinh k h} \left[ \cosh\{k(r\cos\alpha_{j} + z_{0})\} \right] \times \exp\{ikr\sin\alpha_{i}\cos(\theta - \beta_{i})\} \right]_{r_{0} - \Delta r/2}^{r_{0} + \Delta r/2}$$
(13)

Here  $\alpha_i$ ,  $\beta_i$ , and  $r_0$  are the coordinates of the *i*-th current velocity from the coordinate system  $(\alpha, \beta, r)$  shown in **Figure 8** and  $\Delta r$  is the "thickness" of the water volume shown in **Figure 8**. The DWM-II detects the current velocity,  $U_i(t)$ , by taking the average velocity of the water volume defined by  $\alpha_i$ ,  $\beta_i$ , and  $\Delta r$ . The water depth, wave number, angular frequency, wave propagation direction, and height at which the meter is situated above the seabed are represented by h, k,  $\omega$ ,  $\theta$  and  $z_0$ , respectively.

The time lag between the measurement of each velocity component and that of the water surface elevation is designated by  $\Delta t$ .  $\Phi^{-1}$  is the inverse matrix of  $\Phi$  consisting of the cross-spectra between each current velocity,  $U_i(t)$ ;

$$\Phi = \begin{pmatrix} \phi_{U_1U_1} & \phi_{U_1U_2} & \phi_{U_1U_3} \\ \phi_{U_2U_1} & \phi_{U_2U_2} & \phi_{U_2U_3} \\ \phi_{U_3U_1} & \phi_{U_3U_2} & \phi_{U_3U_3} \end{pmatrix}$$
(14)

Equation (11) is the formula used to estimate the directional spreading by the Extended Maximum Likelihood Method (EMLM-Isobe, et al., 1984). Other methods such as the Bayesian Directional spectrum estimation Method (BDM-Hashimoto and Kobune, 1987) and the Extended Maximum Entropy Principle (EMEP-Hashimoto, et al., 1994) can also be applied to estimate the directional spreading function  $G(\theta|f)$ .

Using  $G(\theta|f)$  as estimated by Equation (11), the power spectrum  $S_{\eta}(f)$  of the free surface displacement,  $\eta(t)$ , can be estimated by:

$$S_{\eta}(f) = \Phi_{U_i U_j}(f) / \int_{-\pi}^{\pi} H_{U_i} H_{U_j} G(\theta|f) d\theta \quad (i = 1, 2, 3)$$
 (15)

Multiplying  $G(\theta|f)$  and  $S_n(f)$  yields the directional spectrum  $S(f,\theta)$ ,

$$S(f,\theta) = S_n(f) G(\theta|f)$$
(16)

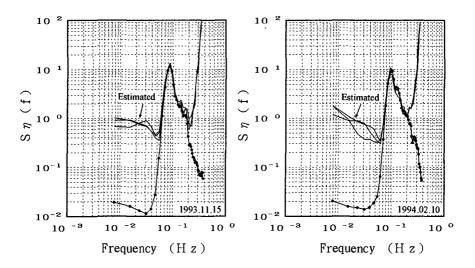


Figure 11 Power Spectra of Free Surface Displacement

Figure 11 shows a comparison between the surface elevation power spectrum measured directly by the ultrasonic waves (indicated by a dotted line) and that obtained from the multiple current velocity components using Equation (15) (indicated by the three thin lines).

Although three power spectra can be estimated from Equation (15), by using i=1,2,3, all of the estimated power spectra show good agreement with the power spectrum measured by the ultrasonic waves around the spectral energy peak.

Figure 12 (a) shows a typical directional spectrum estimated by the EMLM where all of the measured quantities,  $\eta(t)$ ,  $U_1(t)$ ,  $U_2(t)$   $U_3(t)$  were used to estimate the directional spectrum. Figure 12 (b) shows the directional spectrum for the same sea conditions estimated from the three current velocities,  $U_1(t)$ ,  $U_2(t)$   $U_3(t)$ , using the present method without knowledge of the free surface displacement,  $\eta(t)$ . It can be seen that the two spectra compare favorably. The entrance of the experimental observation site faces East and the results clearly show that the waves propagate from the appropriate direction.

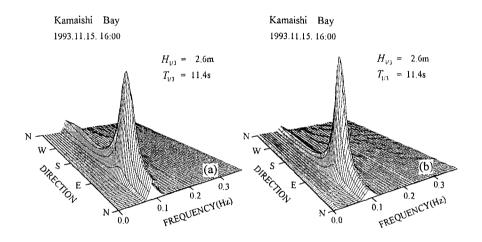


Figure 12 Estimated Directional Wave Spectra

#### Conclusions

Adequate knowledge of sea conditions is essential for clarifying various coastal engineering problems. Difficulties in measuring actual sea conditions, however, have resulted in a lack of critical information. Since the DWM-II can be employed to provide accurate information on directional waves, as well as currents and tides, with only one instrument, it is considered to be one of the most useful measuring systems for conducting research on actual sea conditions. By using techniques introduced in this paper, the auxiliary parameters of the DWM-II can be used to improve its performance. The DWM-II will contribute to increasing the reliability of long-term observations, especially in severe sea states, and will, therefore, lead to the enrichment of our knowledge of realistic sea conditions.

## Acknowledgments

This research was jointly carried out by the Port and Harbour Research Institute, Ministry of Transport, and Japan Marine Surveyors Association under the direction of the Committee for the Development of a Submerged Doppler-Type Directional Wave Meter (Chairman, Professor Y. Goda, Yokohama National University) organized by Japan Marine Surveyors Association. The analyzed field wave data were contributed by the Second Port Construction Bureau, Ministry of Transport. Sincere gratitude is extended to all those involved in this study. We also wish to thank Sidney W. Thurston III, National Sea Grant Fellow of NOAA, who kindly gave us many valuable comments on this research work.

#### References

- Goda, Y., K. Miura and K.Kato (1982): On-Board analysis of mean wave direction with discus buoy, Int. Conf. Wave and Wind Directionality, Paris, Editions Technip, pp.339-359.
- Hashimoto, N. and K. Kobune (1988): Directional spectrum estimation from a Bayesian approach, Proc. 21st ICCE, Spain, Vol. 1, pp. 62-76.
- Hashimoto, N, T. Nagai, K. Sugahara, T. Asai and K. S. Bahk (1993): Surface wave recovery from subsurface pressure record on the basis of weakly nonlinear directional wave theory, Rept. of the Port and Harbour Res. Inst., Vol. 31, No.1, pp.27-51 (in Japanese).
- Hashimoto, N., T. Nagai, and T. Asai (1994): Extension of the maximum entropy principle method for directional wave spectrum estimation, Proc. 24th ICCE, Kobe, Vol. 1, pp. 232-246.
- Isobe, M., K. Kondo and K. Horikawa (1984): Extension of MLM for estimating directional wave spectrum, Proc. Symp. on Description and Modeling of Directional Seas, Paper No. A-6, 15 p.
- Takayama, T., N. Hashimoto, T. Nagai, T. Takahashi, H. Sasaki and Y. Ito (1994): Development of a submerged Doppler-type directional wave meter, Proc. 24th ICCE, Kobe, Vol. 1, pp. 624-634.